

This is the final draft of the contribution published as:

Schubert, M., Kopitz, J., Knöller, K. (2019):

Improved approach for LSC detection of ^{35}S aiming at its application as tracer for short groundwater residence times

J. Environ. Radioact. **208-209**, art. 106022

The publisher's version is available at:

<http://dx.doi.org/10.1016/j.jenvrad.2019.106022>

1 1 Introduction

2 Sustainable abstraction and supply of groundwater is a major socio-economic challenge of our modern
3 society. Both globally growing population and more intensive agricultural activities make the
4 management of groundwater resources a high priority issue. Related policy-based decisions require
5 sufficient knowledge of mean groundwater residence times in exploited aquifers, i.e. mean
6 “groundwater residence times”. The information can be used for estimating the recharge rate of a
7 groundwater resource (Cook and Solomon, 1997) and allows hence assessing (i) the volume of
8 groundwater that can be sustainably abstracted, (ii) groundwater travel times and related matter
9 (contaminant) transport, and (iii) the vulnerability of an aquifer to anthropogenic contamination or
10 climate change. In some cases the assessment of timescales of water-rock interaction processes that
11 might influence the groundwater quality can be of interest as well.

12 A powerful tool for investigating groundwater residence times (as well as groundwater flow and related
13 solute transport processes) is the application of naturally occurring radioisotopes as environmental
14 tracers. Cartwright et al. (2017) reviewed the possibilities and limitations of various radioisotopes (and
15 other residence time tracers) for this purpose. The authors point out that since the groundwater
16 residence time of a specific aquifer may range between a few months and > 1,000,000 years, the half-
17 lives of the applied radioisotopes need to cover a comparable time range. They state that, while the
18 radioisotopes ^3H , ^{14}C , and ^{36}Cl have already been commonly used in the past, general improvements
19 in radio-analytical techniques brought about additional novel approaches that rely on application of the
20 noble gas radioisotopes ^{39}Ar , ^{81}Kr , and ^{85}Kr . The six named radioisotopes cover half-lives between
21 10.76 years (^{85}Kr) and 301,000 years (^{36}Cl) permitting their use for determining groundwater residence
22 times in comparable timescales. However, studies of radioisotopes as tracers that focus on residence
23 times below one year are still scarcely discussed in the literature. In spite of its 12.3 a half-live ^3H
24 might be applicable for detecting sub yearly residence times if the rainfall input function is very well
25 constrained and the detection environment an ideal, i.e., far away from any nuclear source. However,
26 the mandatory high quality data and ideal detection conditions are only rarely available.

27 Innovative approaches that focus on the sub yearly timescale include the application of the natural
28 radioisotopes of radon (^{222}Rn) and beryllium (^7Be). ^{222}Rn starts to build up in any meteoric water (i.e.
29 percolating rain or infiltrating surface water) as soon as it enters the subsurface due to the decay
30 of ^{226}Ra that is omnipresent in any mineral matrix. However, with a half-live of only 3.8 days the ^{222}Rn
31 activity in the infiltrating water reaches secular equilibrium with the ^{226}Ra in soil or aquifer after only

32 about three weeks, which makes ^{222}Rn only applicable for dating very young groundwater (Petermann
33 et al., 2018; Treutler et al., 2007). In contrast, ^7Be with a half-life of 53.1 days allows investigating a
34 much longer time span of up to eight months. It is produced through cosmic ray spallation of oxygen
35 and nitrogen atoms within the upper atmosphere (Cooper et al., 1995). After its production it sticks to
36 aerosols and gets washed out of the atmosphere mainly by precipitation (or settles by dry deposition).
37 As soon as the rainwater seeps into the ground its exposure to cosmic rays stops and the ^7Be decay
38 in the water is not supported by ^7Be production anymore making its decreasing activity concentration
39 (in relation to its activity concentration in the fresh rainwater) an indicator of the groundwater residence
40 time. However, ^7Be has a high tendency to sorb on organic phases, oxyhydrides and oxides; a
41 substantial share of the dissolved beryllium is held back by soil particles and vegetation (Landis et al.,
42 2014; Kaste et al., 2012), which limits its applicability as quantitative aqueous tracer.

43 A natural radionuclide that covers a comparable time range and could hence be alternatively applied
44 as tracer is ^{35}S (Cooper et al., 1995). Just as ^7Be it is continually produced in the upper atmosphere
45 (by cosmic ray spallation of atmospheric ^{40}Ar). After its production it rapidly oxidizes to $^{35}\text{SO}_4^{2-}$, gets
46 dissolved in meteoric water and is finally transferred with the rain to the subsurface. ^{35}S activities in
47 precipitation can be as high as ca. 65 mBq/l (Urióstegui et al., 2015). There are no significant natural
48 sources of ^{35}S in the subsurface (Cooper et al., 1995). Hence its activity concentration in the meteoric
49 water starts to decrease by decay as soon as the water seeps into the ground.

50 In contrast to beryllium SO_4^{2-} is highly mobile in groundwater and is hence not retarded by any mineral
51 substrate. It displays very low reactivity and consequently a geochemical stability over a wide range of
52 hydrochemical conditions. Under oxic and slightly reducing conditions sulfate is transported with the
53 groundwater flow conservatively (Knöller et al., 2005). Under stronger reducing conditions, sulfate may
54 be subject to bacterial reduction provided a bioavailable electron donor such as dissolved organic
55 carbon is supplied (Knöller et al., 2008, Knöller and Schubert, 2010). If sulfate reducing conditions are
56 prevailing, $^{35}\text{SO}_4^{2-}$ is likely to be affected by bacterial degradation in the same way as the stable
57 isotope species of the sulfate molecule. If bacterial sulfate reduction is occurring, the application of
58 the ^{35}S method is limited because of the fact that fractionation factors that might have to be used to
59 correct the ^{35}S analytical results for potential degradation have not been investigated to date.
60 However, bacterial sulfate reduction predominantly affects deep aquifer systems with high apparent
61 groundwater residence times of several years to decades that can a priori not be investigated with
62 the ^{35}S method, anyway.

63 ^{35}S is a β -emitter (decaying to ^{35}Cl) and can be measured by liquid scintillation counting (LSC). Its half-
64 life of 87.4 days makes it a potentially useful tracer for investigating groundwater residence times on
65 timescales of up to 1.2 years. Studies on ^{35}S as an age tracer are scarce; those that exist are often
66 limited to high geographical elevations where snowmelt is the dominant hydrological recharge event;
67 thus simplifying the annual ^{35}S input function to the peak snowmelt (Shanley et al., 2005; Mitchel et al.,
68 2000; Sueker et al. 1999; Cooper et al., 1995).

69 In contrast, ^{35}S concentrations in rainwater, i.e., in more moderate climate regions, may vary
70 significantly even on short timescales of hours to days, resulting in a more involved ^{35}S input function.
71 Furthermore the ^{35}S input function can be significantly affected by seasonal variations in rain intensity
72 (and thus recharge). This constraint necessitates the recording of extended ^{35}S time series, both in
73 rainwater and groundwater, for sound data interpretation in moderate climate zones. Furthermore,
74 groundwater in moderate climate zones may show high SO_4^{2-} concentrations resulting in relatively
75 low ^{35}S activities compared to the total SO_4^{2-} load of the sample in contrast to SO_4^{2-} loads in
76 snowmelt. Analysing ^{35}S in waters with high SO_4^{2-} concentrations is generally challenging if a
77 conventional LSC approach is applied (Urióstegui et al., 2015). The above named challenges limit the
78 range of potential applications of ^{35}S as indicator for groundwater residence times in moderate climate
79 zones (Clark et al., 2016).

80 Finally, it shall be pointed out that pre-concentration of ^{35}S is required for LSC counting since the low
81 natural concentrations of ^{35}S in rain and groundwater necessitate large original water sample volumes.
82 Urióstegui et al. (2015) suggested about 100 mg SO_4^{2-} as adequate load for sound ^{35}S detection by
83 means of LSC and recommended accordingly a sample volume of 20 liters as appropriate for most
84 meteoric waters. In practice, exchange resins are used to pre-concentrate SO_4^{2-} from the original
85 water sample. The resin is subsequently eluted with aqueous NaCl solution and sulphate is
86 precipitated by adding BaCl_2 . This rather laborious sample preparation includes some steps that need
87 to be improved.

88 The objective of this study was to develop, test and present an improved LSC based method that
89 allows the detection of ^{35}S pre-concentrated from natural water samples that contain a wide range of
90 SO_4^{2-} concentrations (up to 1500 mg) in a less labour-intensive way. The study aimed at the
91 optimization of sample preparation, LSC setup and measurement protocol. All measurements were
92 carried out with the liquid scintillation counter TriCarb 3170 Tr/SL.

93

94 2 Material and methods

95 After precipitation of ^{35}S containing SO_4^{2-} from aqueous solution as BaSO_4 a TriCarb 3170 Tr/SL liquid
96 scintillation counter was used for the determination of the ^{35}S activity of the precipitate. The activity
97 was measured after the homogeneous suspension of the ultra-fine-grained BaSO_4 particles in Insta-
98 Gel Plus scintillation cocktail as described by Uriostegui et al. (2015).

99 With the aim to substantially improve the signal-to-noise-ratio of the measurement results, the
100 optimization potential of three independent LSC detection options was investigated. Besides
101 (i) optimization of the LSC counting window, two special features of the TriCarb 3170 Tr/SL, namely
102 (ii) pulse decay discrimination and (iii) pulse index-based background reduction were examined for
103 LSC performance improvement. The so called „figure of merit“ (FOM), i.e. the ratio of
104 efficiency squared and background ($\text{FOM} = \epsilon^2 / B$), was used to quantify the performance
105 improvements. Furthermore, the quenching due to elevated BaSO_4 loads in the sample (and hence in
106 the LSC vial) and the potential spill over of ^{226}Ra counts into the ^{35}S counting window were
107 investigated and quantified.

108 For the execution of test measurements under varying conditions three sets of standards were
109 produced (as described in detail in sect. 3). Each of the three sets contained seven individual
110 standards with increasing SO_4^{2-} loads between 50 and 1500 mg (as described in detail in sect. 3).
111 Standards with SO_4^{2-} loads higher than 1500 mg were not investigated because the corresponding
112 volume of BaSO_4 was too large for the applied 20 ml LSC vials. Each of the seven standards of the
113 first set was spiked with a ^{35}S activity of 290 Bq. The seven standards of the second set were all
114 spiked with a ^{226}Ra activity of 1.1 Bq each. The seven standards of the third set were unspiked.

115

116 3 Experimental

117 3.1 Production of standards

118 Three sets of LSC standards were produced; set #1, set #2 and set #3. Each set contained seven
119 individual standards with increasing loads of ^{35}S -dead SO_4^{2-} (as BaSO_4), namely 50mg, 100mg,
120 250mg, 500mg, 750mg, 1000mg and 1500mg SO_4^{2-} . Hence, 21 standards were produced in total.
121 Each standard of set #1 was spiked with ^{35}S ; each standard of set #2 was spiked with ^{226}Ra (for
122 evaluating the spill over of ^{226}Ra counts into the ^{35}S counting window; see below for details). The
123 standards of set #3 were not spiked at all but contained only ^{35}S -dead BaSO_4 in increasing
124 concentration.

125 Highly water soluble Na_2SO_4 was used to prepare the standards. It was measured by both gamma
126 spectrometry and LSC for any containing radioactivity prior to sample preparation and only Na_2SO_4
127 was used that was free of any ^{35}S . BaCl_2 was used for the preparation of the standards to precipitate
128 SO_4^{2-} as BaSO_4 . It was also tested for radioactivity and the tests revealed low but detectable amounts
129 of ^{226}Ra , which was accounted for in the setup of the experiments and in the assessment of the
130 experimental results (see sect. 3.3).

131 Three sets of Na_2SO_4 standard solutions were made by pipetting from a saturated Na_2SO_4 stock
132 solution (i.e. 170 g/L at 20 °C) into 50 mL centrifuge vials. Each of the three sets comprised seven
133 individual standards with increasing Na_2SO_4 loads that matched the range of SO_4^{2-} loads given
134 above. The standards of set #1 and set #2 were subsequently spiked with 10 μL of a $^{35}\text{SO}_4^{2-}$ stock
135 solution ($\text{Na}^{35}\text{SO}_4$; carrier free) and 2 mL of an aqueous ^{226}Ra stock solution, respectively. That
136 resulted in activity concentrations of about 290 Bq ^{35}S in each vial of set #1 and about 1.1 Bq ^{226}Ra in
137 each vial of set #2. (The aqueous standard $\text{Na}^{35}\text{SO}_4$ and ^{226}Ra stock solutions were obtained from the
138 PTB - National Metrology Institute, Germany and Hartmann Analytic, Germany, respectively.) The
139 seven standards of set #3 were not spiked at all but served as background standards representative
140 for the increasing SO_4^{2-} loads.

141 Subsequently distilled water was added to each of the 21 centrifuge vials in order to equalize the
142 individual volumes to 15 ml for each of the standards. All solutions were acidified with five drops of 6M
143 HCl to a pH of 2.5. In order to quantitatively precipitate the dissolved SO_4^{2-} as BaSO_4 the vials were
144 placed in water filled beakers and heated in the water bath to nearly 100°C before adding a volume of
145 35 mL 0.5M aqueous BaCl_2 solution to each of the vials. After allowing about 12 hours for the BaSO_4
146 to precipitate quantitative precipitation was checked by visual examination of the supernatant solution
147 after adding a few more drops of 0.5M BaCl_2 solution. Since no additional sulphate precipitation was
148 observed in any of the vials quantitative precipitation was assumed.

149 The vials were centrifuged for 10 min at 4000 rpm, the supernatant water was removed with a pipette
150 and the precipitate was washed with distilled water. This washing process was repeated once more.
151 Then the vials were centrifuged again, the supernatant water was tested for neutrality and removed
152 with a pipette. Then the precipitate was dried within the vials at about 100°C to complete dryness (for
153 at least two hours). The resulting dry clumps of BaSO_4 precipitate were next quantitatively transferred
154 into 20 mL LSC vials and weighted for recovery and potential loss of SO_4^{2-} during standard
155 preparation. We used plastic vials instead of glass vials because they display a lower background than

156 glass vials due to their lower intrinsic radioactivity (no traces of ^{40}K). Plastic also has a lower density
157 resulting in a lower probability of particle/photon interactions with the vial wall. Finally, a glass rod was
158 used to pulverize the precipitate directly in the LSC vials.

159 Insta-Gel Plus (PerkinElmer) was chosen as the scintillation cocktail that is most suitable for
160 the purpose. Due to its typical gel formation it allows the homogeneous distribution of suspended
161 solids (such as BaSO_4 powder) within the counting. Therefore, it is ideal for counting the
162 $\text{Ba}^{35}\text{SO}_4$ precipitate.

163 The BaSO_4 powder was suspended in 5 mL distilled water by shaking the vials for homogenization.
164 Subsequently 6.5 mL Insta-Gel Plus were added to each vial and the vials were shaken again. Finally,
165 another 6.5 mL Insta-Gel Plus were added, and the vials were shaken homogenization and gelation
166 were complete. A total volume of 13 ml of Insta-Gel Plus are needed of 5 ml water aqueous
167 suspensions are to be measured because gel formation is dependent on a proper water/cocktail ratio.
168 Prior to the actual LSC measurement the vials were refrigerated for about 30 min in order to reduce
169 the counting background (pers. comm. Richard K. Bibby, Lawrence Livermore National Laboratory,
170 Livermore, USA). Measurement of refrigerated samples results in a reduction of the counting
171 background because it reduces chemoluminescence. Furthermore gel formation of the sample/cocktail
172 mixture is temperature-dependent. Since a refrigerated LSC counter is used, it is recommended that
173 the stability of the gel is tested by cooling the sample prior to counting.

174

175 3.2 Optimization of the counting window

176 For optimization of the counting window LSC measurements were carried out with the standard sets
177 #1 and #3 (i.e. ^{35}S and background). After measuring the actual standards with a certain energy
178 window, the "Replay" option of the TriCarb was used for iterative optimization of the window (the
179 "Replay" option allows re-evaluation of the raw count data based on different evaluation settings
180 without any additional measurement of an individual sample). The variable window settings that were
181 iteratively tested covered the complete range from 0 keV up to the theoretical endpoint of the ^{35}S - β -
182 spectrum at 167keV.

183

184 3.3 Pulse decay discrimination (PDD)

185 A general increase in radiation background with increasing BaSO_4 load was observed for all three sets
186 of standards. That suggested the BaCl_2 , added for the sake of BaSO_4 precipitation from the aqueous

187 solutions, as potential background radiation source. Barium and radium are both members of the
188 alkaline-earth metal group and thus chemically similar, so that substitution of barium by radium is
189 possible. Adding BaCl₂ for preparation of the standards may hence result in a contamination of the
190 standards with radium. That assumption is backed by Urióstegui et al. (2015) who found substantial
191 amounts of radium in several investigated BaCl₂ batches. Not only the counts of the ²²⁶Ra itself but
192 also the counts of its short-lived progeny may spill over into the ³⁵S counting region resulting in higher
193 backgrounds there. In particular the alpha emissions of ²²²Rn, ²¹⁸Po, ²¹⁴Po, ²¹⁰Po can be
194 misinterpreted as ³⁵S decay events (Urióstegui et al., 2015).

195 A gamma spectrometry analysis of the used BaCl₂ batch confirmed the presence of ²²⁶Ra and thus
196 also its short-lived progeny. The measurement was carried out by low-level gamma-spectrometry
197 based on the distinct ²²⁶Ra gamma emission energy of 186.1 keV. (Due to the purity of the BaCl₂ a
198 contribution of ²³⁵U - 185.7 keV - to the peak area could be ruled out.) For the measurements a coaxial
199 Low-Energy HPGe detector, n-type (ORTEC) with an active volume of 39 cm³ and a 0.5 mm Be
200 window was applied. Detector and measuring geometry were calibrated using the certified reference
201 material IAEA-RGU1. Two samples of the used BaCl₂ batch were measured for about 24 h in 150 cm³
202 cylindrical capsules. Spectra analysis was performed with the software Gamma-W[®].

203 Since the ²²⁶Ra radiation background of the ³⁵S-dead BaSO₄ precipitate could not be avoided due to
204 its origin, pulse decay discrimination (PDD) was used to reduce contribution of this background to the
205 overall counts of the measurements. PDD is based on the length of the pulse that is recorded in the
206 electronic circuits of the liquid scintillation counter. Pulses induced by an alpha decay have a longer
207 tailing than those from a beta decay (Buchtela et al., 1974; Thorngate et al., 1974). PDD classifies all
208 detected counts as either alpha or beta events based on the respective pulse length.

209 The homogeneously suspended BaSO₄ particles result in a strong influence of self-absorption. Hence,
210 the use of classical spill-over plots, as they are routinely applied for samples that are homogeneously
211 dissolved in a cocktail, appeared not appropriate for optimization of the PDD discriminator setting. We
212 therefore followed a strategy that considers the spill-over of alpha-decays derived from ²²⁶Ra and its
213 short lived progeny as „additional background“ and applied the FOM to determine the optimum PDD
214 setting. For calculation of the sulphate-load specific FOM values, the standards of set #1 (³⁵S spiked)
215 were applied to determine the individual counting efficiencies (ε), while the standards of set #3 were
216 measured for quantification of the associated ³⁵S-dead backgrounds (B).

217

218 3.4 Pulse index discrimination

219 A very effective method to reduce the overall background in TriCarb instruments is pulse index
220 discrimination, which reduces photomultiplier crosstalk. Photomultiplier crosstalk may occur if natural
221 radioactivity (^{40}K) or cosmic radiation induces the release of photons by the Cerenkov Effect in one of
222 the two photomultipliers (PMT). These photons might also arrive at the second PMT thereby fulfilling
223 the coincidence counting condition. Consequently these events are recorded by the instrument as real
224 counts. However, detailed analysis of the pulses (pulse index discrimination) allows distinguishing
225 Cerenkov events from liquid scintillation events thereby enabling correction for these background
226 signals (Passo and Kessler, 1992). In combination with the BGO guard used in low level counters as
227 the TriCarb 3170 Tr/SL it also targets background scintillation counts caused by external radiation
228 (e.g. cosmic radiation) (Noakes and Valenta, 1996).

229 Since high energetic beta events in the cocktail may induce pulse indices that resemble background
230 counts, the possibility to attenuate the pulse index correction for measuring high-energetic nuclides by
231 increasing the so called „delay-before-burst“ (DBB) time was introduced. However, since ^{35}S is
232 relatively low-energetic and, as in our case, by self-absorption quenched to even lower energies, an
233 improvement of the counting sensitivity by fine-tuning the DBB time appeared unlikely. Still, another
234 study suggested a significant improvement by increasing the DBB time for measuring BaSO_4
235 precipitates (Hong and Kim, 2005). We therefore also tested the effects of longer DBB times.

236

237 4 Results

238 4.1 Production of standards

239 The SO_4^{2-} recovery check by weight confirmed the quantitative recovery of the sulphate that was
240 added to the individual standard solutions as dissolved Na_2SO_4 . In particular, the transfer of the
241 BaSO_4 precipitate from the centrifuge vial into the LSC vial as dry clump simplified the handling of the
242 material considerably. In the LSC vials the BaSO_4 clumps could be easily and completely pulverized
243 with a glass rod allowing a homogeneous distribution of the powder within the scintillation gel.

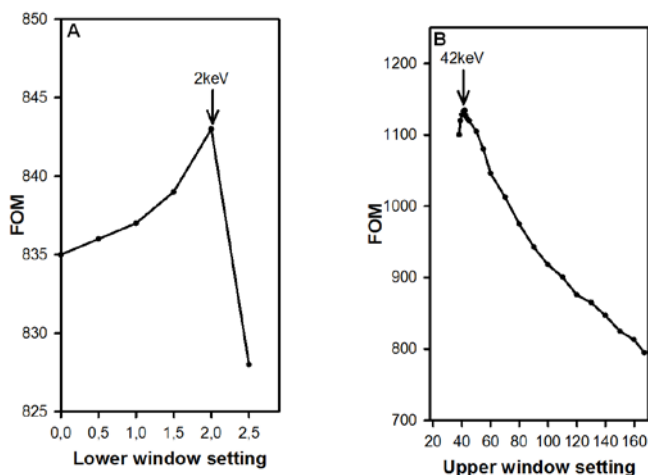
244 It shall also be pointed out that homogeneous distribution of the pulverized BaSO_4 precipitate in the
245 gel filled vials leads to a significantly better counting efficiency than collecting the precipitate on a
246 translucent filter and counting the included ^{35}S on this filter applying a liquid LSC cocktail (e.g. Ultima
247 Gold LLT) without chemical dissolution of the filter (as suggested by Hong and Kim, 2005).
248 Furthermore it shall be mentioned that it is important to add the aqueous spike solutions (^{35}S

249 and ^{226}Ra) not to the LSC vials at the end of the standard preparation process (e.g. with the 5 mL
250 distilled water that are added prior to the Insta-Gel Plus) but rather to the aqueous solutions prior to
251 the BaSO_4 precipitation. Both ^{35}S and ^{226}Ra need to be amalgamated within the particles of the
252 BaSO_4 precipitate for sound determination of the individual quench.

253

254 4.2 Optimization of the counting window

255 A representative example of the results of the measurements and the subsequent replay runs that
256 were carried out with sets #1 (^{35}S) and #3 (background) aiming at the optimization of the counting
257 window is displayed in Fig. 1. For the four standards with sulphate loads between 50 and 250 mg
258 highest FOMs were found in energy windows with a lower window limit ranging between 2.5 and
259 3.5 keV and an upper limit ranging between 42 and 43 keV. For the three standards with sulphate
260 loads between 500 and 1500 mg the highest FOMs were found with a lower window limit between
261 0.0 and 0.5 keV and an upper window limit between 35 and 39 keV.



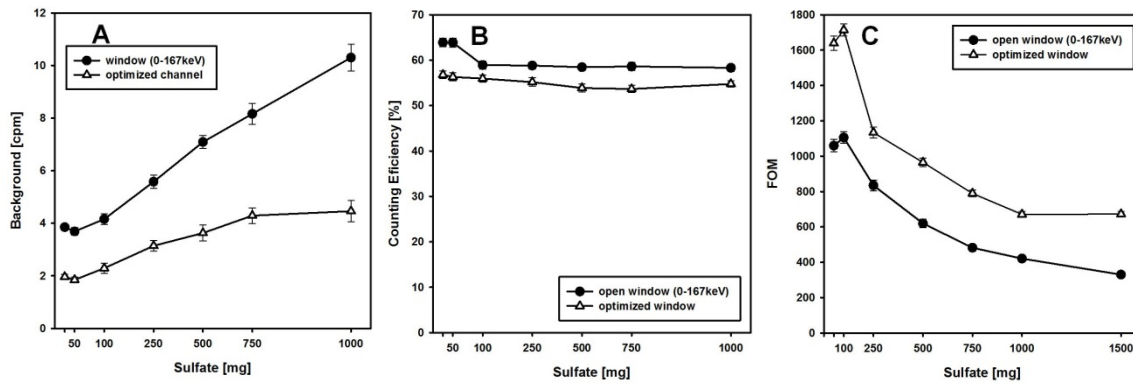
262

263 Fig. 1: Optimizing the energy window setting; ^{35}S -dead standards containing increasing loads of
264 BaSO_4 (set #3) were used as background standards, while standards spiked with ^{35}S (set #1) were
265 applied to determine counting efficiencies, both at different window settings. As an example window
266 optimization is displayed for the standards with a SO_4^{2-} load of 250mg. (A) Lower window limit was
267 increased stepwise and ϵ^2/B (FOM) was calculated. (B) Upper channel setting was lowered stepwise
268 with optimized lower channel until a maximum for the FOM was reached.

269

270 The counting windows that yielded the highest FOMs at the individual sulphate loads are compiled in
271 Tab. 1. While generally the background increases with the sulphate load (as expected), the application
272 of the optimized window settings resulted in a substantial background reduction for all individual

273 standards of the ^{35}S -dead set #3 (Fig. 2A). Although narrowing the counting window causes generally
 274 a slight decrease in counting efficiency (Fig. 2B) as determined with standard set #1, a distinct
 275 increase of the FOM could be achieved for all sulphate loads due to the more decisive background
 276 reduction (Fig. 2C).
 277



278
 279 Figure 2: Effect of window optimization on counting performance at different SO_4^{2-} loads;
 280 (A) Background with open window (i.e. 0 - 167 keV) vs. optimized channel as given in Tab. 1.
 281 (B) Counting efficiency with open window vs. optimized channel. (C) FOM with open window vs.
 282 optimized channel.

283
 284 Table 1: Effect of window optimization on Figure of Merit (FOM)

Sulphate [mg]	FOM open window	FOM optimized (channel setting)
50	1060	1645 (3-43keV)
100	1106	1714 (3-42keV)
250	835	1134 (3-42keV)
500	620	969 (0-39keV)
750	482	799 (0-37keV)
1000	421	671 (0-35keV)
1500	330	672 (0-35keV)

285
 286 Based on this data set we suggest an optimum window setting of 3 - 42 keV for samples containing up
 287 to 500 mg sulphate („low sulphate“) and a window setting of 0 - 37 keV for samples with sulphate
 288 loads above 500 mg („high sulphate“) as a compromise for routine measurements. These settings

289 were retained for all subsequent measurements. As mentioned above, sulphate loads higher than
290 1500 mg are not feasible due to practical considerations.

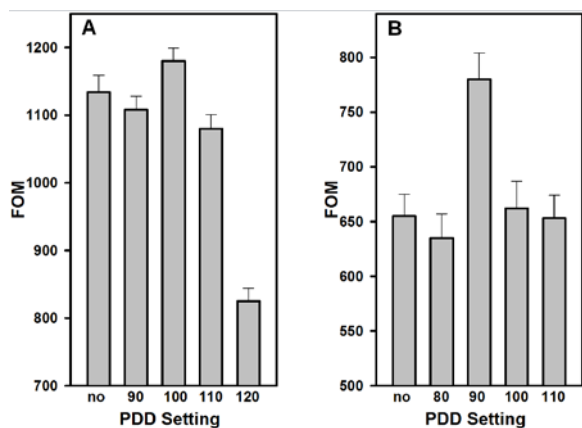
291

292 4.3 Pulse decay discrimination (PDD)

293 The gamma spectrometry measurement revealed a ^{226}Ra activity of the used BaCl_2 of 5 ± 0.4 Bq/kg.
294 Even though this activity concentration is comparably low for commercially available BaCl_2 batches
295 (Uriostegui et al., 2015), the ^{226}Ra -derived counts (i.e. the counts from ^{226}Ra and its short-lived
296 progeny, namely the alpha emitters ^{222}Rn , ^{218}Po , ^{214}Po and the beta emitters ^{214}Pb and ^{214}Bi) are the
297 major cause of the increasing background that was observed for higher BaSO_4 loads.

298 FOM measurements at different PDD discriminator settings were executed with the standard sets #1
299 and #3. Based on the results optimal PDD settings (as indicated by the highest FOM) were determined
300 for “low” (<500 mg) and “high” (>500 mg) sulphate loads (cf. sect. 4.2). They were found to be PDD
301 100 and 90, respectively (Fig. 3). Applying these settings on the ^{226}Ra spiked standards of set #2
302 resulted in a reduction of about 50% of the ^{226}Ra -derived counts in the optimized ^{35}S energy window
303 (cf. sect. 4.2) as compared to measurements without PDD (Supplementary figure S1)) in the open
304 window.

305



306

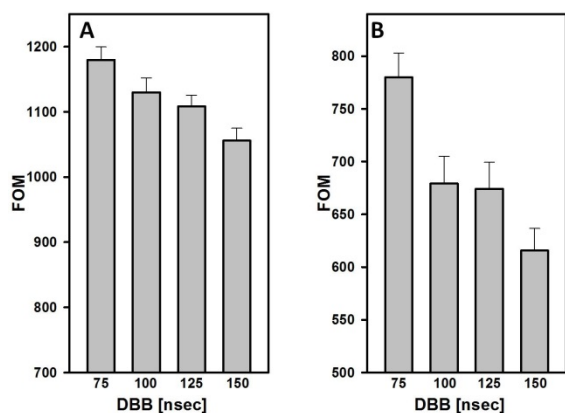
307 Figure 3: Effect of Pulse Decay Discrimination (PDD) on FOM; exemplary results for (A) a low (250mg)
308 and (B) a high sulphate load (1500mg) at the respective optimized channel settings

309

310 4.4 Pulse index discrimination

311 Hong and Kim (2005) suggested a DBB value of 200 ns to maximize the FOM for ^{35}S measurements
312 in aqueous samples in 10ml/10ml proportions with Ultima Gold LLT as scintillation cocktail. Still, the
313 application of Insta-Gel Plus for ^{35}S determination in BaSO_4 as discussed here may necessitate a

314 different setting. In our measurements the shortest possible DBB time of 75ns, which is the default
 315 setting of the TriCarb recommended for measuring low energetic nuclides such as ^3H or also ^{14}C
 316 (whose E_{max} is very close to ^{35}S), was found to give the best results (Fig. 4).



317
 318 Figure 4: Effect of different Delay Before Burst (DBB) times exemplary results for (A) a low (250mg)
 319 and (B) a high sulphate load (1500mg) at the respective optimized channel settings

320
 321 5 Discussion

322 5.1 Recommendation of a detection setup

323 Based on the achieved data, we recommend settings as given in Tab. 2 for counting ^{35}S -containing
 324 BaSO_4 precipitates in the gel-forming Insta-Gel Plus cocktail the. Results for different amounts of
 325 sulphate measured under these conditions are given in Tab. 3.

326
 327 Table 2: Recommended instrument settings for counting ^{35}S -containing BaSO_4 suspensions in Insta-
 328 Gel Plus

	Sulphate load 0-499 mg	Sulphate load 500-1500 mg
Counting mode	Low level	Low level
Counting window	3 - 42 keV	0 - 37 keV
Pulse decay discriminator	100	90
Delay before burst	75 nsec	75 nsec

329
 330
 331

332 Table 3: Counting performance at optimized settings according to Table 2

Counting conditions	Sulphate load [mg SO ₄ ²⁻]	Background [cpm]	Efficiency [%]
	50	2.15	56.7
„Low sulphate“	100	2.20	56.2
	250	2.35	56.2
„High sulphate“	500	2.86	52.9
	750	3.22	52.6
	1000	3.26	53.3
	1500	3.69	53.6

333

334 With optimized settings the counting efficiencies were in the range of 50 - 60 % indicating that quench
 335 correction is necessary for dpm or Bq reporting. External standardization with a γ -emitting ¹³³Ba source
 336 (tSIE or SIS value), as conventional method, appears not suitable for BaSO₄ precipitates, since it
 337 records chemical and colour quenching but cannot quantify the amount of self-absorption in the
 338 particles, resulting in so called „physical quench“ (cf. sect. 5.2). We therefore recommend quench
 339 correction where the (known) amount of BaSO₄ in the sample is correlated to the counting efficiency
 340 as determined with a comparable standard spiked with Ba³⁵SO₄. The efficiencies shown in Tab. 3
 341 indicate that the quench level remains close to constant for a rather large range of SO₄ loads. Thus, in
 342 practice, it might be sufficient to determine the counting efficiency for “low” and “high sulphate”
 343 samples only once and proceed from the assumption that the quench level is practically constant over
 344 either of the two sample ranges. In the case of our detection setup one could assume a counting
 345 efficiency of about 56% for “low” and 53% for “high sulphate” concentrations.

346

347 5.2 Background information related to quench correction

348 The use of ³⁵S as a tracer in groundwater studies requires extremely sensitive procedures that allow
 349 detecting the low ³⁵S levels present in the samples. The processing of large water sample volumes
 350 includes the removal of other naturally occurring radioisotopes from the samples by ion-exchange
 351 chromatography and the pre-concentration of the ³⁵S by Ba³⁵SO₄ precipitation as an absolute
 352 prerequisite (e.g. Urióstegui et al., 2015).

353 Liquid scintillation counting is the method of choice to measure ^{35}S activities. However, LSC
354 measurement of low energetic β -emitters like ^{35}S customarily requires samples in a solution that is
355 homogeneously miscible with the scintillation cocktail. Measuring solid samples is generally hampered
356 by self-absorption. An approach to circumvent the latter limitation is the use of gel-forming scintillation
357 cocktails that allow the measurement of small particles as microsuspension in a stable gel. Carbonate
358 precipitation has been used for a long time to measure ^{14}C as $\text{Ba}^{14}\text{CO}_3$ (Larson, 1973). Likewise,
359 sulphate precipitation with BaCl_2 can be applied to concentrate ^{35}S -sulphate from high water volumes
360 for measurement in a liquid scintillation counter that can accommodate a maximum sample/cocktail
361 mixture of 20 ml. However, with this approach a considerable influence of self-absorption in the
362 suspended particles (“physical quenching”) has to be taken into account. The major contribution to the
363 loss of counting efficiency (“total quenching”) will be caused by self-absorption rather than by chemical
364 and colour quenching as known from homogeneous liquid sample/cocktail mixtures.

365 The by far most commonly applied method to measure and correct for the influence of the latter is
366 standardization with an external γ -source (L’Annunziata, 2012). In the case of TriCarb counters the
367 shift of a Compton spectrum generated by a ^{133}Ba source is applied to quantify chemical and colour
368 quench of a sample and expressed as the so called “tSIE-value” (Kessler, 1991). However, since the
369 generation of Compton-electrons mainly occurs in the liquid cocktail phase of a microemulsion and
370 only to a negligible part inside the particles, the tSIE does not reliably measure physical quench by
371 self-absorption in the particles. We therefore do not recommend the tSIE value for quench correction
372 of BaSO_4 precipitates.

373 In principle, the “Spectral Index of the Sample” (SIS), which detects quench by recording the shift of
374 the sample spectrum towards lower energies would be applicable for recording physical quench,
375 provided the quench curve is set up with ^{35}S -containing BaSO_4 suspensions in Insta-Gel Plus.
376 However, for low level measurements statistical accuracy of this quench indicator is too low.

377 Best results were achieved when counting efficiencies were determined with standards mimicking the
378 sample composition, i.e. the BaSO_4 load.

379

380 5.3 Impact of the BaSO_4 particle size on the counting efficiency

381 We found higher counting efficiencies compared to reports from other groups (Hong and Kim, 2005;
382 Urióstegui et al., 2015), in particular for higher BaSO_4 loads. As mentioned above, the major cause of
383 loss of counting efficiency is self-absorption in the BaSO_4 -particles. Since self-absorption is highly

384 dependent on the particle size, we took special care during preparation of our standards to produce
385 particles for the final measurement that were as small as possible. Therefore, this seems to be the
386 most plausible explanation for our higher counting efficiencies. Likewise, we did not see a striking
387 decrease of counting efficiency with increasing BaSO₄ loads. For chemical quenching a reduction of
388 counting efficiency would be expected for higher loads of the quenching agent. However, no
389 compounds that could cause chemical quenching are present in our standards. The BaSO₄ present in
390 particles does not contribute to chemical quenching and the amount of water is constant for all BaSO₄
391 loads. The decreasing counting efficiencies at higher BaSO₄ loads observed in the former reports
392 might hence rather be due to an increasing size of the BaSO₄ particles with higher BaSO₄ loads
393 resulting in stronger physical quench. If the particle size remains unchanged with an increasing BaSO₄
394 load the influence of physical quenching should remain close to constant, as observed in our study.
395 Furthermore it shall be pointed out that very high BaSO₄ loads might lead to light scattering at the
396 particles which could reduce the amount of photons that reach the photomultipliers of the LSC
397 instrument. We observed an influence of this effect with sulphate loads above 1500 mg and therefore
398 recommend not exceeding this limit (besides the fact that the corresponding volume of BaSO₄ is
399 inappropriate for the applied 20 ml LSC vials). Altogether careful preparation the standards resulted in
400 close to constant counting efficiencies over broad ranges of sulphate load, thereby enabling simple
401 standardization for dpm/Bq reporting.

402

403 5.4 Minimizing of spill-over from α -emitters

404 The optimization of the window setting had a major impact on the signal-to-noise ratio, as quantified by
405 the increase of the FOM. Optimal window settings not only reduce that natural background, but also
406 help to prevent spill-over of counts, in particular from ²²⁶Ra and its progeny, into the ³⁵S window. The
407 lower energy regions of the β -emitters ²¹⁴Pb and ²¹⁴Bi will always overlap with any setting of the ³⁵S
408 window. Consequently, setting the window as narrow as possible will help to reduce background
409 originating from these ²²⁶Ra daughter nuclides. If unquenched, the α -emitting daughters should appear
410 above the maximum energy of ³⁵S. However, α -particles are much more affected by self-absorption as
411 β -electrons. Since quenching of a α -emitter results in a shift of the α -peak to lower energies, self-
412 absorption is likely to cause a spill in to the ³⁵S window. Therefore, especially lowering the upper limit
413 of the ³⁵S-window helps to reduce α -derived background.

414 In addition, the PDD-based α/β -option helps to reduce remaining α -spill. The improvement of the
415 signal-to-noise ratio by applying this option clearly indicates that α -spill can contribute to the
416 background counts, even in the optimized window.

417

418 5.5 Background information related to the delay-before-burst setting

419 All measurements in our study were conducted in the low-level count mode of an instrument that is
420 equipped with a BGO guard. This count mode provides efficient background reduction by applying
421 pulse-index-discrimination to reduce background originating from events outside the cocktail, mainly
422 caused by Cerenkov-effects in the detection chamber, e.g. by the interaction of cosmic radiation with
423 components of the detection chamber or by ^{40}K contaminations (Roessler et al., 1991). The method is
424 based on the observation that each β -event that is registered by the photomultipliers is followed by a
425 number of after-pulses. The pulse-index is defined by the number of after-pulses that are registered in
426 the photomultiplier. Since most of the background events that occur outside the cocktail produce more
427 after-pulses than the β -events in the cocktail, the pulse-index can be applied to reduce this kind of
428 background. The low-level count mode applies most stringent pulse-index discrimination, and is
429 therefore the method of choice for low-level measurements. However, the delay after a β -event that is
430 defined in order to distinguish between true β -events within the cocktail and external events, depends
431 on the counting conditions, in particular on the energy of the β -particles and the used cocktail.
432 Therefore this “delay-before-burst” (DBB) can be adjusted (Passo and Kessler, 1993).

433 Prolongation of the DBB time becomes e.g. necessary when using long fluorescence lifetime (“slow”)
434 scintillation cocktails that produce a significantly delayed signal, i.e. cocktails that contain di-
435 isopropylnaphthalene (e.g. Ultima Gold LLT) in combination with higher energy β -emitters (Salonen et
436 al., 2012). Insta-Gel Plus does not belong to the “slow” cocktails since it is based on 1,2,4-
437 trimethylbenzol. In contrast to Hong and Kim (2005) who used Ultima Gold LLT in their study, the
438 shortest possible DBB time was found to be the best setting for measuring strongly quenched ^{35}S in
439 the Insta-Gel Plus cocktail.

440

441 6 Conclusion

442 A powerful tool for investigating groundwater residence times is the application of naturally occurring
443 radioisotopes as environmental tracers. Commonly applied radioisotopes (^3H , ^{14}C , ^{36}Cl , ^{39}Ar , ^{81}Kr , ^{85}Kr)
444 are suitable for covering water residence times ranging between a few years and over one million

445 years. The omnipresent natural radionuclide ^{35}S adds perfectly to this set of tracers since it is
446 applicable for investigating groundwater residence times of up to 1.2 years. However, the very low
447 activity concentration of ^{35}S in groundwater is challenging. In addition, its concentration in rainwater
448 (^{35}S input function) may vary substantially even on short timescales. These challenges can be met by
449 optimizing both sample preparation procedure and LSC measurement protocol. Improved sample
450 preparation focusses on the homogeneous suspensions of fine-grained ^{35}S -containing BaSO_4 in the
451 Insta-Gel Plus scintillation cocktail. The improvements in instrument setting include the LSC counting
452 window, the pulse decay discriminator setting and the delay before burst setting. Numerous
453 experiments resulted in related recommendations. The recommended settings allow the measurement
454 of low activity concentrations of ^{35}S , which was previously pre-concentrated from natural water
455 samples, containing SO_4^{2-} loads of up to 1500 mg with a reasonably high statistical reliability.

456

457 REFERENCES

- 458 Blume, H.P., Brümmer, G.W., Horn, R., Kandeler, E., Kögel-Knabner, I., Kretschmar, R., Stahr, K.,
459 Wilke, B.M., 2010. Scheffer/Schachtschabel: Lehrbuch der Bodenkunde. Springer Berlin/Heidelberg,
460 p. 121.
- 461 Buchtela, K., Tschurlovits, M., Unfried, E., 1974. Eine Methode zur Untersuchung von α - und β -
462 Strahlen in einem Flüssigszintillationsgerät. *Int. J. Appl. Radiat. Isot.* 25, 551-555.
- 463 Cartwright, I., Cendón, D., Currell, M., Meredith, K., 2017. A review of radioactive isotopes and other
464 residence time tracers in understanding groundwater recharge: Possibilities, challenges, and
465 limitations. *Journal of Hydrology* 555, 797-811.
- 466 Clark, J.F., Urióstegui, S.H., Bibby, R.K., Esser, B.K., Tredoux, G., 2016. Quantifying Apparent
467 Groundwater Ages near Managed Aquifer Recharge Operations Using Radio-Sulfur (^{35}S) as an
468 Intrinsic Tracer. *Water* 8(11), 474-485.
- 469 Cook, P., Solomon, D.K., 1997. Recent advances in dating young groundwater:
470 chlorofluorocarbons, ^3H , ^3He and ^{85}Kr . *Journal of Hydrology* 191, 245-265.
- 471 Cooper, L.W., Olsen, C.R., Solomon, D.K., Larsen, I.L., Cook, R.B., Grebmeier, J.M., 1991. Stable
472 isotopes of oxygen and natural and fallout radionuclides used for tracing runoff during snowmelt in an
473 Arctic watershed. *Water Resour. Res.* 27, 2171-2179.
- 474 Edler, R., Passo, C., 2010. LSC Application note: Basics of alpha/beta Discrimination for Liquid
475 Scintillation Counting. PerkinElmer LAS (Germany) GmbH, 63110 Rodgau-Jügesheim.

476 Hong, Y., Kim, G., 2005. Measurement of Cosmogenic ^{35}S Activity in Rainwater and Lake Water.
477 Anal. Chem. 77, 3390-3393.

478 Johnson, D.R., Smith, J.W., 1963. Glass filter paper suspension of precipitates for liquid scintillation
479 counting. Anal. Chem. 35, 1991-1992.

480 Kaste, J.M., Baskaran, M., 2012. Meteoric ^7Be and ^{10}Be as process tracers in the environment.
481 In: Baskaran, M. (Ed.), Handbook of Environmental Geochemistry. Springer, Berlin, Heidelberg, 61-85.

482 Kessler, M.J., 1991. Application of quench monitoring using transformed external standard spectrum
483 (tSIE). in: Liquid Scintillation Counting and Organic scintillators. Lewis Publishers, Chelsea, MI, pp.
484 647-653.

485 Knöller, K., Trettin, R., Strauch, G., 2005. Sulphur cycling in the drinking water catchment area of
486 Torgau-Mockritz (Germany): insights from hydrochemical and stable isotope investigations. Hydrol.
487 Process. 19 (17), 3445- 3465.

488 Knöller, K., Vogt, C., Feisthauer, S., Weise, S.M., Weiß, H., Richnow, H.H., 2008. Sulfur cycling and
489 biodegradation in contaminated aquifers: insights from stable isotope investigations. Environ. Sci.
490 Technol. 42 (21), 7807- 7812.

491 Knöller, K., Schubert, M., 2010. Interaction of dissolved and sedimentary sulfur compounds in
492 contaminated aquifers. Chem. Geol. 276 (3-4), 284 - 293.

493 L'Annunziata, M.F., 2012. External standard quench-indicating parameters In: Handbook of
494 radioactivity analysis. Academic Press Amsterdam, The Netherlands, pp. 438-446.

495 Landis, J.D., Renshaw, C.E., Kaste, J.M., 2014. Quantitative retention of atmospherically deposited
496 elements by native vegetation is traced by the fallout radionuclides ^7Be and ^{210}Pb . Environ. Sci.
497 Technol. 48, 12022-12030.

498 Larsen, P.O., 1973. A convenient method for liquid scintillation counting of barium carbonate- ^{14}C . Int.
499 J. Appl. Radiat. Isot. 24, 612-613.

500 Michel, R.L., Campbell, D., Clow, D., Turk, J.T., 2000. Timescales for migration of atmospherically
501 derived sulphate through an alpine/subalpine watershed, Loch Vale, Colorado. Water Resour. Res.
502 36, 27-36.

503 Noakes, J.E., Valenta, R.J., 1996. The role of $\text{Bi}_4\text{Ge}_3\text{O}_{12}$ as an auxiliary scintillator for a/b/g liquid
504 scintillation counting and low level counting. in Cook, G.T., Harkness, D.D., MacKenzie, A.B., Miller,
505 B.F., Scott, E.M. (Eds.), Advances in Liquid Scintillation Spectrometry. Radiocarbon Publishers,
506 University of Arizona, Tuscon, pp. 283-92.

507 Passo, C.J., Kessler, M.J., 1992. Selectable delay before burst - a novel feature to enhance low-level
508 counting performance. in: Noakes, J.E., Schönhofer, F., Polach, H.A. (Eds), *Advances in Liquid*
509 *Scintillation Spectrometry*. Radiocarbon Publishers, University of Arizona, Tuscon, pp. 67-74.

510 Petermann, E., Gibson, J.J., Knöller K., Pannier, T., Weiß H., Schubert, M., 2018. Determination of
511 groundwater discharge rates and water residence time of groundwater-fed lakes by stable isotopes of
512 water ($\delta^{18}\text{O}$, $\delta^2\text{H}$) and radon (^{222}Rn) mass balances. *Hydrological Processes* 32/6, 805-816.

513 Salonen L., Kaihola L., Carter B., Cook G.T., Passo C., 2012. Low-level counting theory. in: *Handbook*
514 *of radioactivity analysis*, Academic Press Amsterdam, The Netherlands, pp. 625-634.

515 Shanley, J.B., Mayer, B., Mitchell, M.J., Michel, R.L., Bailey, S.W., Kendall, C., 2005. Tracing sources
516 of streamwater sulphate during snowmelt using S and O isotope ratios of sulphate and ^{35}S activity.
517 *Biogeochemistry* 76, 161-185.

518 Sueker, J.K., Turk, J.T., Michel, R.L., 1999. Use of cosmogenic ^{35}S for comparing ages of water from
519 three alpine/subalpine basins in the Colorado Front Range. *Geomorphology* 27, 61-74.

520 Thorngate, J.H., McDowell, W.J., Christian, D.J., 1974. An application of pulse shape discrimination to
521 liquid scintillation counting. *Health Physics* 27, 123-126.

522 Treutler, H.C., Just, G., Schubert, M., Weiß H., 2007. Radon as tracer for the determination of mean
523 residence times of groundwater in decontamination reactors. *J. Radioanal. Nucl. Chem.* 272, 583-588.

524 Urióstegui, S.H., Bibby, R.K., Esser, B.K., Clark, J.F. 2015. Analytical Method for Measuring
525 Cosmogenic ^{35}S in Natural Waters: *Anal. Chem.* 87, 6064-6070.

526 Roessler, N., Valenta, R.J., van Cauter, S., 1991. Time-resolved liquid scintillation counting. in:
527 Ross, H., Noakes, J.E., Spalding, J.D., *Liquid Scintillation Counting and Organic Scintillators*. Lewis
528 Publishers Inc., Stockport UK, pp. 501-511.

529 Salonen, L., Kaihola, L., Carter, B., Cook, G.T., Passo C.J., 2012. Environmental liquid scintillation
530 analysis: Background reduction methods - Instrument considerations. Academic Press Amsterdam,
531 The Netherlands, pp. 627-633.